



HAL
open science

Trafficking properties and activity regulation of the neuronal glycine transporter GLYT2 by protein kinase C

Amparo Fornés, Enrique Núñez, Pablo Alonso-Torres, Carmen Aragón,
Beatriz López-Corcuera

► To cite this version:

Amparo Fornés, Enrique Núñez, Pablo Alonso-Torres, Carmen Aragón, Beatriz López-Corcuera. Trafficking properties and activity regulation of the neuronal glycine transporter GLYT2 by protein kinase C. *Biochemical Journal*, 2008, 412 (3), pp.495-506. 10.1042/BJ20071018 . hal-00478857

HAL Id: hal-00478857

<https://hal.science/hal-00478857>

Submitted on 30 Apr 2010

HAL is a multi-disciplinary open access archive for the deposit and dissemination of scientific research documents, whether they are published or not. The documents may come from teaching and research institutions in France or abroad, or from public or private research centers.

L'archive ouverte pluridisciplinaire **HAL**, est destinée au dépôt et à la diffusion de documents scientifiques de niveau recherche, publiés ou non, émanant des établissements d'enseignement et de recherche français ou étrangers, des laboratoires publics ou privés.

Trafficking properties and activity regulation of the neuronal glycine transporter GLYT2 by protein kinase C

Amparo Fornés, Enrique Núñez, Pablo Alonso-Torres, Carmen Aragón, and Beatriz López-Corcuera¶

Departamento de Biología Molecular and Centro de Biología Molecular “Severo Ochoa”, Consejo Superior de Investigaciones Científicas-Universidad Autónoma de Madrid, 28049-Madrid, Spain.

¶To whom correspondence should be addressed:

Beatriz López-Corcuera,
Departamento de Biología Molecular,
Centro de Biología Molecular “Severo Ochoa”,
C/ Nicolás Cabrera 1
Universidad Autónoma de Madrid, 28049-Madrid, Spain.
Telephone number: 34 91 1964631
Fax number: 34 91 91-1964420
e-mail: blopez@cbm.uam.es

The abbreviations used are: DAT, dopamine transporter; ERK, extracellular signal-regulated kinases; GABA, γ -amino butyric acid; GAT1, GABA transporter 1; GFP, green fluorescent protein; GLYT1 and GLYT2, glycine transporters 1 and 2; HBS, HEPES-buffered saline; JNK, c-Jun NH₂-terminal kinases; MAPK, mitogen-activated protein kinases; MDCK, Madin-Darby canine kidney; MEK, MAP/ERK kinase; NET, norepinephrine transporter; NFPS, N[3-(4'-fluorophenyl)-3-(4'-phenylphenoxy)-propyl]sarcosine; NHS-SS-biotin, sulfo-succinimidyl 2-(biotinamido) ethyl-1,3-dithiopropionate; PI3K, phosphatidylinositol 3-OH kinase; PKC, protein kinase C; PMA, 4 α -phorbol 12 myristate 13-acetate; SERT, serotonin transporter; SLC6, solute carrier 6; TfR, transferrin receptor.

Running title: Regulation of GLYT2

Key words: glycine, transport, GLYT2, phorbol ester, protein kinase C, trafficking

The neuronal glycine transporter GLYT2 controls the availability of the neurotransmitter in glycinergic synapses and the modulation of its function may influence synaptic transmission. Active transporter is located in membrane rafts and reaches the cell surface through intracellular trafficking. Here we prove that GLYT2 constitutively recycles between the cell interior and the plasma membrane by means of a monensin-sensitive trafficking pathway. Besides, a regulated trafficking can be triggered by 4 α -phorbol 12-myristate 13-acetate (PMA). We demonstrate that PMA inhibits GLYT2 transport by causing net accumulation of the protein in internal compartments through an increase of the internalization rate. In addition, a small increase of plasma membrane delivery and a redistribution of the transporter to non-raft domains is triggered by PMA. A previously identified phorbol ester-resistant mutant (K422E) displaying an acidic substitution in a regulatory site, exhibits constitutive traffic but, in contrast to wild type, fails to show glycine uptake inhibition, membrane raft redistribution and trafficking modulation by PMA. We prove that the action of PMA on GLYT2 involves protein kinase C (PKC)-dependent and independent pathways, although an important fraction of the effects are PKC-mediated. We show the additional participation of signaling pathways triggered by the small GTPase Rac1 on PMA action. GLYT2 inhibition by PMA and monensin take also place in brainstem primary neurons and synaptosomes, pointing to a GLYT2 trafficking regulation in the central nervous system.

INTRODUCTION

Glycine is the major inhibitory neurotransmitter in posterior areas of the vertebrate central nervous system [1]. The availability of the neurotransmitter in glycine-mediated synapses is controlled by Na⁺ and Cl⁻-dependent plasma membrane glycine transporters belonging to the SLC6 family [2]. The two glycine transporter isoforms, GLYT1 and GLYT2, display differential thermodynamic features, complementary cellular distributions and *in vivo* roles [3-7]. The neuronal transporter GLYT2 is mainly involved in the synaptic recycling of glycine to preserve the quantal glycine content inside synaptic vesicles, and it assists GLYT1 in regulating glycine levels at synapses [8]. GLYT2 deficient mice die prematurely during the second postnatal week displaying severe neuromotor alterations due to impaired inhibitory glycine transmission [7]. In addition, hypofunction of glycine signalling has been implicated in several pathologies such as neuromotor disorders, nociceptive pain or epilepsy, and recently, it was shown that some missense mutations in the gene encoding GLYT2 cause hyperekplexia or startle disease in humans [9]. Therefore, increasing the efficacy of inhibitory glycine transmission would conceivably produce benefits in these disorders and it is reasonable to speculate that the modulation of GLYT2 activity might find therapeutic applications [8]. However, despite the essential role of GLYT2, the effects of the exogenous modulation of its activity on glycinergic function are presently unknown, as are the mechanisms that regulate GLYT2 activity *in vivo*. Consequently, the study of GLYT2 regulation may help to understand the role of this transporter in glycinergic physiology and pathologies.

The SLC6 transporters are believed to be tightly regulated, the PKC-mediated regulation being one of the most studied mechanisms (see 10-14, for a review). Several lines of evidence indicate that activation of PKC by phorbol esters such as PMA or by stimulation of membrane receptors coupled to the phospholipase C-PKC pathway, leads to acute reduction in transport activity and membrane expression of the monoamine transporters and the GABA transporter GAT-1 among other members of the family [10,13]. This seems to be due to a net increase of the internalization rate of the plasma membrane residing transporters [15-17], although additional down regulation of catalytic efficiency by PMA has been verified for the serotonin transporter [18,19].

We have previously shown that PMA inhibits GLYT2 transport activity and induces a decrease in plasma membrane transporters [20]. However, the detailed effects of PMA on GLYT2 trafficking and the signalling mechanisms that underlie PMA action

on GLYT2 have not been studied. In this report we focus on the trafficking properties of GLYT2 and demonstrate the existence of a monensin-sensitive constitutive traffic and a PMA-regulated traffic. PMA inhibition is caused by a removal of the transporter from the plasma membrane through an increase of the internalization rate and a lower increase of plasma membrane delivery, resulting in a net accumulation of the protein in internal compartments. A PMA-resistant mutant harboring K422E, an acidic substitution in the recently identified regulatory site around Lys-422 of GLYT2 [20], fails to show glycine uptake inhibition, membrane raft redistribution and trafficking modulation by PMA, but exhibits constitutive traffic. In addition, we show that GLYT2 down regulation by PMA is mainly, but not exclusively, due to PKC activation. The involvement of alternative signal transduction cascades in transporter inhibition by PMA has been explored.

EXPERIMENTAL

Materials

Wistar rats were bred at the 'Centro de Biología Molecular S.O.' (Madrid, Spain) following current policies for the use of animals in neuroscience research. [2-³H] Glycine (1.6 TBq/mmol) was from PerkinElmer Life Science. Ligase and restriction enzymes were from Roche Molecular Biochemicals. NHS-SS-biotin was obtained from Pierce. Okadaic acid, PMA, staurosporin, GF109203X, FTP inhibitor III, Rac1 inhibitor, U0126, PD98059, SB203580, PD169316, SP600125, LY292002 and U73122 were from Calbiochem (San Diego, CA). Peroxidase-linked anti-rabbit IgG and ECL reagent were from GE Healthcare. Antibodies were from the following sources: Calnexin, Stressgen (Canada); Transferrin receptor (TfR), Zymed Laboratories Inc. (San Francisco, CA); Flotillin-1, Transduction Laboratories (Lexington, KY); Caveolin, Abcam (Cambridge, UK). The secondary antibodies coupled to fluorophores were from Molecular Probes (San Diego, CA). GLYT2 antibodies against the N-terminus were previously characterized [21]. GLYT2 inhibitor ORG25543 [22] was generously donated by Dr. Zoran Rankovic (Organon, Scotland, UK). GLYT1 inhibitor N[3-(4'-fluorophenyl)-3-(4'-phenylphenoxy)-propyl]sarcosine (NFPS) was a generous gift of Dr. Jesús Benavides (Sanofi-Aventis, Vitry sur Seine, France). All other reagents were obtained from Sigma-Aldrich (St. Louis, MO).

Site-directed mutagenesis

GLYT2 substitution mutants were generated by site-directed mutagenesis using the method of Higuchi as previously described [23] using primers from Isogen (The Netherlands). At least two independent *Escherichia coli* colonies carrying the mutant plasmids were characterized by sequencing and transport activity. GLYT2 or K422E in fusion with GFP in the pEGFPC1 vector were constructed as described (GFP-GLYT2, [24]).

Cell growth and protein expression

COS7 or MDCK cells (American Type Culture Collection) were grown at 37 °C and 5% CO₂ in high glucose Dulbecco's modified Eagle's medium supplemented with 10% fetal bovine serum. Transient expression was performed using LipofectAMINE Plus (COS7 cells) or LipofectAMINE 2000 (MDCK cells) from Invitrogen, following the supplier's procedures. Reproducible results were obtained with 60-70% confluent cells on a 100 mm dish using 4 µg of total DNA. Cells were incubated for 48 or 72 h at 37°C until used.

Primary cultures of brainstem neurons

Brainstems from 16 day old rat fetuses were isolated in HBSS buffer (Invitrogen, San Diego, CA), and dissociated with activated papain (Papain Dissociation System, Worthington, Lakewood, NJ). The cells were resuspended in plating buffer (NB/B27 50:1 by vol, from Invitrogen; 0.5 mM glutamine; 0.05 mg/ml gentamicin; 0.01% streptomycin; 100 mU/ml penicillin G; and containing 5% fetal calf serum). The cells were plated on poly-L-lysine (13 µg/ml) coated 24-well plates at a density of 300,000 cells/well (for transport assays) or 40,000 cells/well on coverslips (immunofluorescence). Each day, half the well volume was replaced with fresh plating buffer without serum.

Glycine transport assay

Transport assays in COS7 cells or primary brainstem neurons were performed at 37°C (unless otherwise indicated) in HEPES-buffered saline (HBS: 150 mM NaCl, 10 mM HEPES-Tris, pH 7.4, 1 mM CaCl₂, 5 mM KCl, 1 mM MgSO₄, 10 mM glucose) containing 2 µCi/ml [³H]-labeled glycine (1.6 TBq/mmol; NEN Life Science Products),

as described [20]. In COS7 cells, transport solution was isotopically diluted at 10 μ M final glycine concentration, and transport measured by subtracting the glycine accumulation by mock-transfected COS7 cells (about 0.3 nmol gly/mg protein/6 min, representing around 20% of the glycine transport by wild type GLYT2) from that of the transporter cDNA transfected cells and normalized by the protein concentration. In primary brainstem neurons, the transport solution contained, in addition to the labeled glycine, 5 μ M NFPS, and 2 mM of α -(methylamino) isobutyric acid, L-Pro, L-Val, L-Ala and L-Leu, to lower background glycine accumulation. GLYT2-mediated glycine transport in neurons was defined as sensitive to ORG25543 (100 nM), and normalized for the protein concentration. All assays were performed in triplicate.

Immunofluorescence and confocal microscopy

Transfected MDCK cells were subjected to immunofluorescence as described [20] using rabbit or rat primary antibodies against the N-terminus of GLYT2 together with mouse anti-transferrin receptor. Secondary antibodies were anti-rabbit or anti-rat antibodies coupled to Alexa 488 fluorophore for GLYT2 and anti-mouse coupled to Alexa 555 for TfR. Alternatively, cells were transfected with GLYT2 fused to GFP in the pEGFPC1 vector (GFP-GLYT2, [24]) and fixed with 4% paraformaldehyde in PBS. The cells were visualized by confocal microscopy on a Microradiance BioRad using a vertical Axioskop 2 microscope (Zeiss) or LSM510 META coupled to an inverted microscope AXIOVERT200 (Zeiss).

Pharmacological treatments

Acute treatments: Transfected or mock-transfected COS7, MDCK cells or primary brainstem neurons were serum-starved for 3 h at 37°C and then incubated in HBS at 37°C during 30 min (if not otherwise indicated in the figure legends) with vehicle, monensin (20 μ M) or PMA (0.01-1 μ M), alone or with the indicated additions. All the compounds were freshly prepared and protected from light. Cells were then extensively washed, and fixed for immunofluorescence labeling, assayed for glycine transport activity or solubilized for lipid raft isolation. Chronic PMA treatment: Transfected or mock-transfected COS7 cells were incubated overnight (16h) with 1 μ M PMA in culture medium, washed with HBS, and serum starved for 3h in this medium. Subsequent acute PMA treatment was performed as above.

Cell surface labeling

Surface labeling in steady-state conditions was performed as described [20,25] by maintaining the samples at 4°C during all the steps. Transfected or mock transfected cells, were washed 3x with HBS, allowed to stand for 15 min, and incubated for 20 min with 1.5 mg/ml sulfo-NHS-SS-biotin. Wells were washed twice with 100 mM L-lysine in HBS, and incubated in the same medium for 45 min. Cells were scraped (scraping buffer in mM: Tris, 50; NaCl, 150, PMSF, 0.4; pepstatin, 0.004; pH 7.4), quantified for protein concentration and equal amounts of protein were lysed during 30 min by supplementing the buffer with 5 mM EDTA, 1% Triton-X100, 0.1% SDS, and 0.25 % sodium deoxycholate. After cell debris removal, an aliquot was brought to 1x Laemmli buffer (total fraction). To the remaining lysate, 40 µl of prewashed streptavidin-agarose beads (Sigma) were added and incubated for 2h at room temperature with end-over-end shaking. Beads were pelleted and biotinylated proteins were eluted with Laemmli buffer. Samples were run on a 7.5% SDS-PAGE gel, subjected to Western blot with ECL detection and quantified on a GS-710 Calibrated Imaging Densitometer from Bio-Rad (Hercules, CA) with Quantity One software by using film exposures in the linear range as described [19]. Control load was performed by calnexin reprobings of Western blot membranes.

Delivery of GLYT2 transporters to the plasma membrane

Biotinylation under trafficking-permissive conditions was carried out as above but cells were rinsed with HBS prewarmed at 37°C prior to incubation with sulfo-NHS-SS-biotin for the desired times at this temperature in the presence of 1 µM PMA or vehicle [26]. Protein trafficking was stopped by placing the cells on ice and all the subsequent steps including rinsing with HBS and residual biotin quenching were performed at 4°C and samples processed as above. An aliquot of the cells was treated in parallel with sulfo-NHS-SS-biotin at 4°C to determine initial surface protein.

Internalization of GLYT2 transporters

Reversible biotinylation was performed as described [27]. COS7 cells were surface labelled at 4°C as above and part of the biotinylated cells were washed and kept at 4°C to provide a measure of the total pool of cell surface transporter available for internalization and strip efficiencies. The rest of the cells were washed with prewarmed

(37°C) HBS supplemented with bovine serum albumin 0.2% and glucose 0.18% (HBSbg) and incubated at 37°C for 2 min. Endocytosis was allowed to proceed for varying periods of time at 37°C in the absence/presence of 1 μ M PMA or vehicle. Traffic was stopped by placing plates in an ice bath and washing 2x with ice-cold HBS. Residual cell surface biotin was stripped with freshly prepared NT buffer (50 mM MesNa, 150 mM NaCl, 1 mM EDTA, 0.2% bovine serum albumin, 0.18% glucose, 20 mM Tris, pH 8.6) during 25 min. In this conditions we observed a residual surface biotin of about 10%. Cells were lysed and processed as above.

Isolation of detergent-resistant membranes

Membrane rafts from transfected MDCK cells or from rat brainstem synaptosomes were isolated according to standard procedures [28] with variations. Scraped washed cells or purified synaptosomes were lysed at 2 mg protein/ml in MBS buffer: 25 mM MES and 150 mM NaCl, pH 6.5, containing 0.5% Triton X-100 and protease inhibitors (PMSF 0.4 mM + Sigma cocktail) at a detergent/protein ratio of 3.33. Cells were solubilized by incubation during 30 min at 4°C and homogenized in a Dounce homogenizer (10 strokes). Synaptosomal membranes [25] were solubilized by passing them through a 25 gauge needle followed by a 30 min incubation at 4°C. Equal volumes of 80% (w/v) sucrose were added to the lysates and mixed thoroughly. Lysed samples (4 ml) in 40% sucrose were overlaid successively with 4 ml of 30% and 5% sucrose (in MBS+PI) in a SW40 ultracentrifuge tube. After centrifugation at 185000 x g for 18 hr at 4°C, 1 ml fractions were collected from the top. The proteins in each fraction were precipitated with 10% cold trichloroacetic acid, and subjected to 10% SDS-PAGE and immunoblotting.

Data analysis

Non linear regression fits of experimental data were performed with ORIGIN (Microcal Software, Northampton, MA). The effect of inhibitors on uptake was expressed and processed as reported [23]. The kinetic parameters of GLYT2 delivery or internalization to or from the plasma membrane were calculated as described [16] by fitting the time course of biotinylated transporter at 37°C (T_t) to a single exponential equation $T_t = A(1 - e^{-t/\tau})$, where A stands for the maximum band density; t for time (in minutes), and τ stands for the time constant of the process, the inverse of which is a measure of the exo-

or endocytosis rate. Statistical analysis on transport data or band densities were performed using ANOVA with Bonferroni's post hoc analysis or Student's *t* test.

RESULTS

GLYT2 regulated and constitutive traffic

Previous studies by our group showed that GLYT2 expressed either in heterologous systems such as COS7 or PC12 cells or in native systems such as synaptosomes or primary neurons distributes between the cell surface and the intracellular compartment in a proportion that is characteristic of the expression system [20,24,25]. This suggests that the steady-state distribution of the transporter is controlled by a constitutive intracellular traffic, which can be deviated from steady-state conditions by regulatory agents as neuronal activity or phorbol esters [20,24,25]. To establish whether GLYT2 inhibition by PMA involves dynamic trafficking, in the present work we have treated COS7 cells expressing GLYT2 with PMA at traffic-restrictive (18°C) and traffic-permissive (37°C) temperatures and monitored transport activity and transporter membrane expression (Figure 1). As expected, a 30 min incubation with increasing PMA concentrations at 37°C caused a maximal 30-40% reduction of glycine transport by GLYT2 and a parallel decrease in biotinylated transporter together with a raise in intracellular non biotinylated protein (Figure 1B and C). Conversely, there was neither transport inhibition nor loss of plasma membrane GLYT2 when PMA treatment was performed at 18°C, indicating that trafficking of the transporter is needed for the PMA inhibition to take place.

Some SLC6 transporters have been shown to be constitutively internalized and recycled to the plasma membrane. One way to study constitutive protein trafficking is to use the proton ionophore monensin, which collapses the proton gradients that maintain the acidic pH within the intracellular organelles, and interferes with the endosomal trafficking [15]. Figure 2A, B shows that monensin treatment of COS7 cells expressing GLYT2 during 30 min decreased the amount of surface transporter in a comparable manner as did PMA, and the combined addition of both drugs produced a higher plasma membrane GLYT2 down-regulation. Parallel glycine uptake measurements confirmed the loss of functional surface GLYT2 by monensin (Figure 2C). We also studied transporter surface expression by immunofluorescence and confocal microscopy in cells expressing GLYT2. MDCK cells are better tools than COS7 cells for transporter visualization because more GLYT2 is located in basal conditions at the cell surface, and

therefore, vehicle-treated cells showed an intense surface fluorescence (Figure 2D). Monensin treatment dropped the amount of plasma membrane transporter and accumulated the protein in intracellular structures where GLYT2 (green fluorescence) partially co-localized with the endosomal marker transferrin receptor (TfR [29], red fluorescence). As monensin produces a broad endosomal trafficking block, the accumulated intracellular transporter could be due to a recycling blockade but also to a monensin late endosomal trafficking obstruction. However, we did not observe intracellular transporter accumulation in cells treated in parallel with chloroquine (Figure 2D). This, together with the decrease in biotinylated transporter by monensin (Figure 2A, B), strongly suggest that GLYT2 undergoes constitutive recycling and accumulates in intracellular compartments by continuous internalization under recycling blockade.

Effect of PMA on glycine transport and surface expression of GLYT2 wild type and K422E mutant

In a previous study, we identified Lys-422 as a regulatory site of glycine transport activity by GLYT2. The substitution of this residue by acidic amino acids conferred resistance to PMA [20]. Figure 3A and 3B show that PMA treatment of COS7 cells expressing GLYT2 produced a dose and time-dependent inhibition of glycine transport that did not occur in cells expressing K422E. The action of PMA was not a result of non-specific phorbol ester effects, because the inactive analogue 4 α -phorbol 12, 13-didecanoate (4 α -PDD) did not inhibit GLYT2 [20]. Wild type inhibition saturated at concentrations over 50 nM PMA and displays an $IC_{50} = 13.4 \pm 1.8$ nM. The calculated apparent second order rate constant for PMA inhibition was $k = 5.3 \times 10^{-6} \text{ M}^{-1} \text{ s}^{-1}$. At 1 μM PMA, inhibition reached the greatest extent within 1h with a $t_{1/2}$ of 5 min. Hence, PMA treatment produced about 40% reduction in glycine transport by GLYT2 measured at 10 μM glycine, (60% maximal reduction of kinetic parameters V_{max} and K_{m} [20]), while K422E was resistant to the phorbol ester (no V_{max} modification although the K_{m} reduction was still observed [20]).

The above functional data, in agreement with results presented in Figure 1, suggest that GLYT2 V_{max} decrease is due to a PMA-induced removal of the wild type transporter protein from the plasma membrane. In order to inspect the action of PMA on the trafficking features of the K422E mutant, we studied transporter surface

expression by confocal microscopy in MDCK cells expressing GLYT2 transporters fused with the green fluorescent protein (GFP), a construct that was previously characterized [24] (Figure 3C). Treatment with PMA promoted intracellular accumulation of GFP-GLYT2 in about 70-80% of the cells in a comparable extent as did monensin (mon), and a slightly higher effect was observed by the combined addition of both drugs (PMA+mon). PMA-induced intracellular accumulation was also observed in the presence of the phosphatase inhibitor okadaic acid and was reversed by the general kinase inhibitor staurosporin, suggesting the involvement of protein kinases in the action of PMA on GLYT2. Conversely, Figure 3D shows that GFP-K422E mutant did not increase its abundance in the cell interior in response to PMA (only in 5-10% of the cells) despite its low basal membrane expression ([20] and see below). It is of interest to note that K422E mutant was sensitive to monensin, which produced protein accumulation in intracellular compartments (75% of the cells) as did for GLYT2 wild type. This result suggests that mutation of residue Lys-422 abolishes PMA-modulated GLYT2 trafficking but not its constitutive traffic.

Effect of PMA on delivery and internalization rates

Since membrane expression results from a dynamic equilibrium between membrane delivery and internalization, we used modified biotinylation assays to detect protein trafficking to and from the plasma membrane. Transporter delivery to the cell surface was estimated by biotinylating transfected COS7 cells at 37°C in the presence of PMA or vehicle in order to label proteins that cycle through the plasma membrane. Surface labelled transporters were collected on streptavidin agarose beads and subjected to immunoblot with GLYT2 antibodies. Parallel biotinylation assays under non-trafficking permissive conditions (4°C), allowed to measure transporter steady-state surface expression. $20.5 \pm 2.5\%$ of total GLYT2 and $8.4 \pm 2.7\%$ of total K422E were labeled at 4°C, according with the lower membrane expression of the mutant [20]. These values were invariant during the time frames of our experiments (not shown). Figure 4A,B shows representative immunoblots for GLYT2 (A) and K422E (B). In our conditions, the membrane-impermeant biotinylating reagent was unable to label intracellular proteins (less than 8% of total calnexin immunoreactivity in the biotinylated fraction). Within 5 min there was about 2-fold increase in the amount of biotinylated transporters and about 3-fold raise was detected in a plateau reached within 15 min. This time-dependent increase was accompanied by a decrease in the amount of

transporter in the non biotinylated fraction and no change in the total transporter amount. By measuring the amount of ^{37}C -labeled transporter at increasing incubation times over the transporter labeled at 4°C for both wild type and mutant, the delivery rates can be compared [16,26,27]. Average time courses of membrane insertion (Figure 4A,B, lower graphs) were fit by a single exponential function as described in “Experimental”, and estimations of the basal delivery rates were obtained (0.109 ± 0.02 and $0.119 \pm 0.03 \text{ min}^{-1}$ for GLYT2 and K422E, respectively). PMA promoted a modest and similar increase in the estimated exocytosis rates of the two transporters (0.132 ± 0.03 and $0.141 \pm 0.05 \text{ min}^{-1}$), suggesting that mutant resistance to PMA is not related to a differential alteration of the transporters delivery. In addition, under PMA treatment the wild type and mutant recycling transporter pools were increased by about 25-30%.

We next examined GLYT2 transporter internalization using a reversible biotinylation strategy. To do this, surface transporters were labeled with a disulfide bond-containing biotinylating reagent at 4°C and then permitted to internalize (at 37°C) for increasing times in the presence of PMA or vehicle. The transporter labeled at 4°C represents the maximal amount that could be internalized and it is a measure of the steady-state surface protein, which was specific of each GLYT2 transporter (see above). At the end of the internalization time, surface biotin was removed by MesNa, a membrane-impermeant reducing agent, and biotinylated transporters were isolated and quantified. In our experimental conditions, a 85-90% efficiency of biotin stripping was determined by MesNa treatment at 4°C (not shown). Figure 4C, D shows representative immunoblots and densitometric analysis for GLYT2 (C) and K422E (D). A plateau was reached within 15 min in which about 30-35% of surface transporters were protected from MesNa. No further increases in accumulated transporters were observed at higher incubation times, supporting rapid recycling of the internal pool. By fitting the experimental internalization data as above, the basal intracellular accumulation rates were found to be 0.115 ± 0.06 and $0.402 \pm 0.1 \text{ min}^{-1}$ for GLYT2 and K422E, respectively. This indicates a more rapid basal internalization by the mutant, in accordance with its lower membrane expression [20]. PMA treatment accelerated the basal internalization rate of GLYT2 wild type by about 2.5-fold, resulting in an accumulation rate of $0.292 \pm 0.07 \text{ min}^{-1}$ ($n=4$, significantly different from vehicle-treated cells, $p<0.05$ in Student's *t* test), whereas no increase was observed for K422E ($0.460 \pm 0.09 \text{ min}^{-1}$). In addition, no alteration of the endocytosed transporter pool sizes

were detected. Taken together, our delivery and internalization experiments suggest that PMA shifts GLYT2 trafficking, but no K422E mutant traffic, towards internal compartments by increasing endocytosis to a higher extent than exocytosis.

Effect of PMA on transporter association with membrane rafts

We have recently shown that GLYT2 is associated with membrane rafts in the neuronal plasma membrane and that the removal of cholesterol and sphingolipids impairs both raft-association and GLYT2 activity [Núñez et al., unpublished results]. Since the lipid environment may constitute a new mechanism to modulate GLYT2 transporter activity, we wished to examine the effects of PMA on membrane rafts localization. Transporter-expressing MDCK cells were treated with vehicle or PMA at 37°C and then solubilized with Triton X-100 at 4°C. Detergent-resistant membranes were separated by sucrose-density centrifugation (Figure 5). Western blotting of the gradient fractions showed that GLYT2 and K422E mutant were present in membrane raft light fractions (4 and 5) together with the raft marker flotillin-1, whereas proteins excluded from rafts as the TfR were exclusively found in high density fractions. Densitometric analysis of the fractions revealed about $17 \pm 2\%$ of the total GLYT2 and $18 \pm 3\%$ of the total K422E in the light fractions. Treatment of cells with PMA displaced GLYT2 from the raft to the non-raft fractions (9-12) so that only about $1 \pm 0.8\%$ of total transporter remained in light fractions with a concomitant increase in the non-raft fractions. However, the K422E mutant did not show any change in fraction distribution under PMA ($19 \pm 3\%$ in light fractions). Also the localization of the markers flotillin-1 and TfR in the gradient fractions was not altered by PMA.

Protein kinase C involvement in GLYT2 inhibition by PMA

PMA is a potent PKC activator, but there are other cellular phorbol ester receptors that may trigger different signaling cascades including Ras-GRP, chimaerins, Munc13 or protein kinase D [30,31]. In order to know whether the action of PMA on GLYT2 was mediated by PKC, we used pharmacological tools. As shown in Figure 6A, the general serine/threonine and tyrosine kinase inhibitor staurosporin fully reversed the GLYT2 transport inhibition [20], and the trafficking modulation by PMA (see Figure 3C,D). In addition, the bisindolylmaleimide GF109203X, which is the most specific inhibitor of PKC produced a robust, though not total, reversion of glycine transport down regulation (Figure 6B). Furthermore, chronic PMA treatment of COS7 cells, a procedure that

effectively down regulates classic and novel PKC isoforms (Figure 6C, inset), reduced about 40% the inhibition produced by 1 μ M acute PMA on expressed GLYT2 (Figure 6C). These results indicate that PMA action on GLYT2 may involve PKC dependent and independent pathways, although an important fraction of the effects are PKC-mediated. Conversely, PKC does not appear to be involved in constitutive traffic, since the reduction of biotinylated GLYT2 by monensin remained invariant after PKC down regulation (78% and 79% of the vehicle-treated transporter remained at the plasma membrane after monensin in control or chronic PMA, respectively. Figure 6D, inset). In addition, glycine transport inhibition by the ionophore was not significantly modified after PKC down regulation ($40 \pm 7.5\%$ versus $33 \pm 7.1\%$ after chronic PMA, Figure 6D).

We have initiated the search of the signaling pathways that may additionally mediate PMA effects on GLYT2 by examining how the inhibition of key proteins of potentially implicated cascades affects PMA action. The results presented in Figure 7 indicate that pretreatment of COS7 cells expressing GLYT2 with the PKC inhibitor GF109203X produced the maximal decrease in GLYT2 inhibition by PMA ($32 \pm 2.5\%$ became $12 \pm 2.6\%$ inhibition), confirming that PKC activation is the main event involved. However, a significant reduction of PMA action could be observed in the presence of an inhibitor of the small GTPase Rac1 ($32 \pm 2.5\%$ inhibition was reduced to $21 \pm 3.2\%$). Since Rac1 can trigger regulatory cascades of cytoskeletal dynamics [32], this suggests the involvement of such pathways in GLYT2 regulation. Moreover, none of the remaining compounds assayed was able to diminish GLYT2 inhibition by PMA. The inactivation of the Ras exchange factors Ras or Ras-GRP with a farnesyl transferase inhibitor (FTPinhIII) showed no effect on PMA inhibition, indicating that Ras is not upstream of Rac1 in this pathway as described in other systems [32]. This may discard that the activation of the MAPK pathways by Ras could be responsible of PMA-induced GLYT2 down regulation. In addition, due to the reported possibility of MAPK cascade activation by Rac1 signaling [33] we used inhibitors of ERK (U0126 for MEK1/2 and PD98059 for MEK1), p38MAPK (SB203580 and PD169316) and JNK (SP600125). The PMA inhibition was not decreased but even a small increase was detected, suggesting that MAP kinases are not involved in PMA action on GLYT2 (see discussion). Finally, the involvement of PI3K or phospholipase C was discarded as their

respective inhibitors LY292002 and U73122 did not alter the extent of PMA-induced GLYT2 down regulation.

GLYT2 down regulation by monensin and PMA takes also place in brainstem primary neurons and synaptosomes

The COS7 cell heterologous expression system permits to analyze the differential responses by wild type and mutant GLYT2 transporters. However, we wished to know whether the observed constitutive and regulated trafficking properties of GLYT2 were also relevant in a brain-derived preparation. Figure 8A shows that incubation of rat brainstem primary neurons with monensin also decreased the amount of plasma membrane GLYT2 (about 60% of surface protein remained after 15 min-treatment) and its glycine transport was inhibited even with higher potency than in heterologous systems (Figure 8B). In addition, increasing concentrations of PMA produced a dose-response inhibition of endogenous GLYT2 activity (Figure 8C). The IC_{50} for PMA inhibition (19.7 ± 0.6 nM) and the maximal reduction of GLYT2 activity (about 30% at $0.2 \mu\text{M}$ glycine), are comparable to that achieved in the heterologous system (see above). As revealed by Figure 8D, PMA treatment of brainstem neurons decreased kinetic parameters of the glycine transport by GLYT2 more than in COS7 cells. V_{max} was reduced from 9.6 ± 0.8 to 2.7 ± 0.5 nmol gly/mg protein/ 15 min in control and PMA treatments, and K_m decreased from 36.3 ± 7.3 to $16.6 \pm 3.0 \mu\text{M}$. These values represent about 70% and 50% reduction in V_{max} and K_m , respectively. Moreover, isolation of membrane rafts from rat brainstem synaptosomes after PMA treatment demonstrated that GLYT2 present in raft fractions was also displaced to the non-raft fractions by the drug (Figure 8E). According to data in cells (see above), about $12 \pm 3\%$ of the total GLYT2 and $40 \pm 6\%$ flotillin-1 were in the light fractions in basal conditions. Under PMA treatment, only $1 \pm 0.5\%$ of total transporter but $39 \pm 4\%$ of total flotillin-1 remained in raft fractions (Figure 8F). These results suggest that GLYT2 is subjected to regulated and constitutive trafficking and point to a role of PKC in the modulation of the transporter in the central nervous system.

DISCUSSION

Different studies with knockout animals and the investigation of the regulatory properties of neurotransmitter transporters, have lead to the belief that the modulation of

the expression and/or the activity of plasma membrane transporters influences neurotransmission [4-8,12]. In this report we analyze the trafficking features of the neuronal glycine transporter GLYT2 and establish, for the first time, the existence of a constitutive and regulated traffic of the protein. To observe GLYT2 constitutive internalization, we have used the carboxyl ionophore monensin, which blocks recycling by increasing the pH in endosomes [15]. Monensin reduced the amount of surface biotinylated GLYT2 causing a parallel transporter accumulation in TfR-containing endosomes. The intracellular GLYT2 clusters observed by confocal microscopy under monensin treatment could not be mimicked by inhibiting lysosome processing, discarding the interference with the late endosomal trafficking as the main cause of transporter accumulation [34]. Therefore, monensin effect was due to the obstruction of GLYT2 constitutive traffic that, consequently, produced glycine transport inhibition. Besides, we could not discard a marginal direct inhibitory effect of the ionophore on GLYT2 activity, especially in primary neurons [15].

The present study also establishes the requirement of GLYT2 trafficking for PMA regulation as it takes place at 37°C but not at 18°C, a temperature that is expected to produce a considerable inhibition of general trafficking [15, 27]. Traffic involvement was further supported by confocal microscopy and surface biotinylation showing that GLYT2 transporter removed from the plasma membrane was accumulated in internal compartments through an increase of the internalization rate and a lower increase of plasma membrane delivery. The biotinylation of live cells at 37°C has been validated for GLYT2 through parallel measurements of TfR trafficking (not shown) as proven for related plasma membrane proteins [16,26,27,35,36], and by verifying the absence of artifactual GLYT2 internalization by the biotin reagent [15]. By this method, we estimated GLYT2 delivery and internalization rates that are on line with those measured for related transporters in non-neural cells [17,26,35], although trafficking velocities higher than those have been determined for the GAT-1 transporter in neurons [16] probably due to cell-specific mechanisms. It should be noted, however, that our data may represent an overestimation of the transporter delivery due to more efficient protein labeling at 37°C, and an underestimation of its endocytosis rate due to rapid recycling interference [26, 37]. Nevertheless, by estimating in parallel the relative trafficking rates of GLYT2 and a phorbol ester-resistant mutant K422E, the effects of PMA could be compared. We determined a 2.5-fold increase in GLYT2 endocytosis rate under PMA treatment, according with enhancements detected for other transporters [13,16,17,35].

In addition, we measured a delivery increase by PMA that affects both the GLYT2 wild type and the phorbol ester-resistant K422E mutant used in this study [20]. This mutant fails to show transport inhibition, internalization enhancement and membrane raft displacement by PMA, indicative of differential regulatory properties. The up regulation of delivery may explain the net increase in glycine transport by the K422E mutant that was occasionally observed in response to PMA (see Figure 3 and [20]). The response of wild type and mutant to monensin suggests that the mutation of Lys422 abolishes regulated but not constitutive traffic.

Lys422 is a crucial residue for glycine transport that maintains a conformational connection with the glycine binding/permeation site [20]. Based on the high resolution structure of LeuTa, a prokaryotic homologue of the SLC6 transporters [38], it was shown that this residue lays in the amino terminal portion of the fifth transmembrane helix, near the cytoplasmic substrate permeation pathway [39]. This situation is optimal for a regulatory residue and indeed, after its establishment in GLYT2 [20], positions with a regulatory role were described in homologous regions of NET and SERT [35,40]. The simultaneous phosphorylation of two NET residues nearby this position, is linked to PMA-dependent internalization. The substitution of these residues in GLYT2 with neutral or acidic amino acids produces single mutants partially resistant to PMA [20]. The similar properties of NET and GLYT2 mutants anticipate these residues could function as phosphoacceptors also in the latter. The specific roles of phosphorylation within the SLC6 transporters [18,41,42], assures future research.

One interesting question is whether the action of PMA on GLYT2 trafficking accounts for the whole inhibitory effect of GLYT2 transport. Our present data suggest that most of the PMA-induced GLYT2 inhibition is due to surface transporter removal (see Figure 1). However, the diminution in glycine transport V_{max} by PMA was higher (about 60%) than the detected reduction of surface transporter (40%). As PMA displaces GLYT2 from its optimal location in cholesterol-rich membrane rafts, and GLYT2 activity is regulated by the lipid environment [43], the modulation of transporter function may result from both its trafficking regulation and its activity regulation. This could explain a lower V_{max} than expected from surface transporter reduction. Another question is the relationship between membrane raft redistribution and transporter internalization. The fraction of GLYT2 that is raft redistributed, although represents a small percentage of the total transporter (about 15% in synaptosomes), seems to account for the whole amount of transporter present at the

surface (only about 5–10% of total GLYT2 is biotinylated in synaptosomes, and 60% of synaptosomal GLYT2 rafts are surface located, [43]). We propose that internalization may selectively affect to raft-associated GLYT2. Indeed, our unpublished results indicate that M β CD and filipin block PMA action, therefore suggesting that raft location is necessary for PMA internalization.

One important conclusion of this study that remained unanswered to date is the involvement of PKC in GLYT2 inhibition by PMA, and the relevance of this modulation in brain-derived preparations pointing to a GLYT2 trafficking regulation in the central nervous system. Our results indicate that PMA action on GLYT2 may involve PKC-dependent and independent pathways, although an important fraction of the effects are PKC-mediated as in other SLC6 transporters [10,13,15,35]. The involvement of MAPK signaling pathways triggered by Ras exchange factors can be discarded since we did not detect any reduction of PMA inhibition when blocking this upstream step. Instead, we found a minor although reproducible increase in GLYT2 inhibition by PMA in the presence of MAPK inhibitors, suggesting that these cascades may exert a protective effect on GLYT2 as reported for related transporters [44-47]. Conversely, the results presented here indicate that GLYT2 is most likely regulated by signaling pathways triggered by the small GTPase Rac1, which is involved in the regulation of the actin cytoskeleton [32]. It has been shown that Rac1 can be stimulated by PMA either directly or through the upstream action of PKC, and its activity can be regulated by chimaerins, a non-PKC phorbol-ester receptors involved in actin cytoskeleton organization, cell adhesion, cell cycle progression, neurite outgrowth and neural development [30-33,48]. Recently, a SERT association with the actin cytoskeleton through the binding of the LIM adaptor protein Hic-5 preceding PMA-induced transporter internalization has been reported [19]. The involvement of actin cytoskeleton in the regulation of GLYT2 became also apparent from our previous data [20], and deserves upcoming research. In addition, future studies addressing the physiological stimuli that trigger these regulatory pathways will be undertaken to understand the role of GLYT2 in glycinergic neurotransmission

This work was supported by the Spanish ‘Dirección General de Enseñanza Superior e Investigación Científica’ (BMC2002-03502 and BFU2005-05931/BMC), and by the ‘Comunidad Autónoma de Madrid’ (11/BCB/010 and S-SAL-0253/2006), and an institutional

grant from the 'Fundación Ramón Areces'. The group is member of the Network for Cooperative Research on Membrane Transport Proteins (REIT), co-funded by the 'Ministerio de Educación y Ciencia', Spain and the European Regional Development Fund (ERDF; Grant BFU2005-24983-E/BFI). The authors wish to thank Dr. Carlos Sánchez for help with the confocal microscopy.

REFERENCES

1. Aragón, C. and López-Corcuera, B. (2003) Structure, function and regulation of glycine neurotransmitters. *Eur. J. Pharmacol.* **479**, 249-262
2. Chen, N. H., Reith, M.E. and Quick, M. W. (2004) Synaptic uptake and beyond: the sodium- and chloride-dependent neurotransmitter transporter family SLC6. *Pflugers Arch.* **447**, 519-31
3. López-Corcuera, B., Martínez-Maza, R., Núñez, E., Roux, M.J., Supplisson, S. and Aragón, C. (1998) Differential properties of two stably expressed brain-specific glycine transporters. *J. Neurochem.* **71**, 2211-2219
4. Gomeza, J., Hülsmann, S., Ohno, K., Eulenburg, K., Szoke, K., Richter, D. and Betz, H. (2003a) Inactivation of the glycine transporter 1 gene discloses vital role of glial glycine uptake in glycinergic inhibition. *Neuron* **40**, 785-796
5. Tsai, G., Ralph-Williams, R. J., Martina, M., Bergeron, R., Berger-Sweeney, J., Dunham, K. S., Jiang, Z., Barak Caine, S. and Coyle, J. (2004) Gene knockout of glycine transporter 1: characterization of the behavioral phenotype. *Proc. Natl. Acad. Sci. U.S.A.* **101**, 8485-8490
6. Yee, B. K., Balic, E., Singer, P., Schwerdel, C., Grampp, T., Gabernet, L., Knuesel, I., Benke, D., Feldon, J., Mohler, H. and Boison, D. (2006) Disruption of glycine transporter 1 restricted to forebrain neurons is associated with a procognitive and antipsychotic phenotypic profile. *J. Neurosci.* **26**, 3169-81
7. Gomeza, J., Ohno, K., Hülsmann, S., Armsen, W., Eulenburg, V., Richter, D. W., Laube, B. and Betz, H. (2003b) Deletion of the mouse glycine transporter 2 results in a hyperekplexia phenotype and postnatal lethality. *Neuron* **40**, 797-806
8. Aragón, C. and López-Corcuera, B. (2005) Glycine transporters: crucial roles of pharmacological interest revealed by gene deletion. *Trends Pharmacol. Sci.* **26**, 283-286
9. Rees, M. I., Harvey, K., Pearce, B. R., Chung, S. K., Duguid, I. C., Thomas, P., Beatty, S., Graham, G. E., Armstrong, L., Shiang, R., Abbott, K. J., Zuberi, S. M., Stephenson, J. B., Owen, M. J., Tijssen, M. A., van den Maagdenberg, A. M., Smart, T. G., Supplisson, S. and Harvey, R. J. (2006) Mutations in the gene encoding GlyT2 (SLC6A5) define a presynaptic component of human startle disease. *Nat Genet.* **38**, 801-806
10. Zahniser, N. R. and Doolen, S. (2001) Chronic and acute regulation of Na⁺/Cl⁻-dependent neurotransmitter transporters: drugs, substrates, presynaptic receptors, and signaling systems. *Pharmacol. Ther.* **92**, 21-55

11. Mortensen, O. V. and Amara, S. G. (2003) Dynamic regulation of the dopamine transporter. *Eur. J. Pharmacol.* **479**, 159-170
12. Torres, G. E., Gainetdinov, R. R. and Caron, M. G. (2003) Plasma membrane monoamine transporters: structure, regulation and function. *Nat Rev Neurosci.* **4**, 13-25
13. Melikian, H. E. (2004) Neurotransmitter transporter trafficking: endocytosis, recycling, and regulation. *Pharmacology & Therapeutics* **104**, 17-27
14. Robinson, M. B. (2006) Acute regulation of sodium-dependent glutamate transporters: a focus on constitutive and regulated trafficking. *Handb Exp Pharmacol.* **175**, 251-75
15. Sorkina, T., Hoover, B. R., Zahniser, N. and Sorkin, A. (2005) Constitutive and protein kinase C-induced internalization of the dopamine transporter is mediated by a clathrin-dependent mechanism. *Traffic* **6**, 157-170
16. Wang, D. and Quick, M. W. (2005) Trafficking of the plasma membrane gamma-aminobutyric acid transporter GAT1. Size and rates of an acutely recycling pool. *J. Biol. Chem.* **280**, 18703-18709
17. Jayanthi, L. D., Samuvel, D. J. and Ramamoorthy, S. (2004) Regulated internalization and phosphorylation of the native norepinephrine transporter in response to phorbol esters. Evidence for localization in lipid rafts and lipid raft-mediated internalization. *J. Biol. Chem.* **279**, 19315-19326
18. Jayanthi, L. D., Devadoss, J., Samuvel, D. J., Blakely, R. D. and Ramamoorthy, S. J. (2005) Evidence for biphasic effects of protein kinase C on serotonin transporter function, endocytosis and phosphorylation. *Mol. Pharmacol.* **67**, 2077-87
19. Carneiro, A.M. and Blakely, RD. (2006) Serotonin-, protein kinase C-, and Hic-5-associated redistribution of the platelet serotonin transporter. *J Biol Chem.* **281**, 24769-80
20. Fornés, A., Núñez, E., Aragón, C. and López-Corcuera, B. (2004) The second intracellular loop of the glycine transporter 2 contains crucial residues for glycine transport and phorbol ester-induced regulation. *J. Biol. Chem.* **279**, 22934-22943
21. Zafra, F., Aragón, C., Olivares, L., Danbolt, N. C., Giménez, C. and Storm-Mathisen, J. (1995) Glycine transporters are differentially expressed among CNS cells. *J. Neurosci.* **15**, 3952-3969
22. Caulfield, W. L., Collie, I. T., Dickins, R. S., Epemolu, O., McGuire, R., Hill, D. R., McVey, G., Morphy, J. R., Rankovic, Z. and Sundaram, H. (2001) The first potent and selective inhibitors of the glycine transporter type 2. *J. Med. Chem.* **44**, 2679-2682
23. López-Corcuera, B., Núñez, E., Martínez-Maza, R., Geerlings, A. and Aragón, C. (2001) Substrate-induced conformational changes of extracellular loop 1 in the glycine transporter GLYT2. *J. Biol. Chem.* **276**, 43463-43470

24. Geerlings, A., Nunez, E., Rodenstein, L., Lopez-Corcuera, B and Aragon, C. (2002) Glycine transporter isoforms show differential subcellular localization in PC12 cells. *J Neurochem.* **82**, 58-65
25. Geerlings, A., Núñez, E., López-Corcuera, B. and Aragón, C. (2001) Calcium- and syntaxin 1-mediated trafficking of the neuronal glycine transporter GLYT2. *J. Biol. Chem.* **276**, 17584-17590
26. Fournier, K. M., González, M. I. and Robinson, M. B. (2004) Rapid trafficking of the neuronal glutamate transporter, EAAC1: evidence for distinct trafficking pathways differentially regulated by protein kinase C and platelet-derived growth factor. *J. Biol. Chem.* **279**, 34505-34513
27. Loder, M. K. and Melikian, H. E. (2003) The dopamine transporter constitutively internalizes and recycles in a protein kinase C-regulated manner in stably transfected PC12 cell lines. *J. Biol. Chem.* **278**, 22168-22174
28. Ait Slimane, T., Trugnan, G., van Ijzendoorn, S. C. D. and Hoekstra, D. (2003) "Raft-mediated trafficking of apical resident proteins occurs in both direct and transcytotic pathways in polarized hepatic cells: role of distinct lipid microdomains". *Mol. Biol. Cell* **14**, 611-624
29. Sheff, D. R., Daro, E. A., Hull, M. and Mellman, I. (1999) The receptor recycling pathway contains two distinct populations of early endosomes with different sorting functions. *J Cell Biol.* **145**, 123-39
30. Kazanietz M. G. (2002) Novel "nonkinase" phorbol ester receptors: the C1 domain connection. *Mol Pharmacol.* **61**, 759-67
31. Brose, N. and Rosenmund, C. (2002) Move over protein kinase C, you've got company: alternative cellular effectors of diacylglycerol and phorbol esters. *J Cell Sci.* **115**, 4399-4411
32. Burridge, K. and Wennerberg, K. (2004) Rho and Rac take center stage. *Cell* **116**, 167-179
33. Bokoch, G. M. (2003) Biology of the p21-activated kinases. *Annu. Rev. Biochem.* **72**, 743-81
34. Miranda, M., Dionne, K.R., Sorkina, T. and Sorkin, A. (2007) Three ubiquitin conjugation sites in the amino terminus of the dopamine transporter mediate protein kinase C-dependent endocytosis of the transporter. *Mol Biol Cell.* **18**, 313-23
35. Jayanthi, L. D., Annamalai, B., Samuvel, D. J., Gether, U. and Ramamoorthy, S. J. (2006) Phosphorylation of the norepinephrine transporter at threonine 258 and serine 259 is linked to protein kinase C-mediated transporter internalization. *J. Biol Chem.* **281**, 23326-40
36. Lan, J.-Y., Skeberdis, V. A., Jover, T., Grooms, S. Y., Lin, Y., Araneda, R. C., Zheng, X., Bennett, M. V. L. and Zukin, R. S. (2001) Protein kinase C modulates NMDA receptor trafficking and gating. *Nat. Neurosci.* **4**, 382-390

37. Schmidt, A., Hannah, M. J. and Huttner, W. B. (1997) Synaptic-like microvesicles of neuroendocrine cells originate from a novel compartment that is continuous with the plasma membrane and devoid of transferrin receptor. *J. Cell Biol.* **137**, 445-458.
38. Yamashita, A., Singh, S. K., Kawate, T., Jin, Y. and Gouaux, E. (2005) Crystal structure of a bacterial homologue of Na⁺/Cl⁻-dependent neurotransmitter transporters. *Nature.* **437**, 215-23
39. Zhang, Y. W. and Rudnick, G. (2006) The cytoplasmic substrate permeation pathway of serotonin transporter. *J Biol Chem.* **281**, 36213-20
40. Ramamoorthy, S., Samuvel, D. J., Buck, E. R., Rudnick, G. and Jayanthi, L. D. (2007) Phosphorylation of threonine residue 276 is required for acute regulation of serotonin transporter by cyclic GMP. *J. Biol Chem.* **282**, 11639-11647
41. Quick, M. W., Hu, J., Wang, D. and Zhang, H.-Y. (2004) Regulation of a gamma-aminobutyric acid transporter by reciprocal tyrosine and serine phosphorylation. *J. Biol. Chem.* **279**, 15961-15967
42. Grånäs C., Ferrer J., Loland C. J., Javitch J. A., and Gether U. (2003) N-terminal truncation of the dopamine transporter abolishes phorbol ester- and substance P receptor-stimulated phosphorylation without impairing transporter internalization. *J. Biol. Chem.* **278**, 4990-5000
43. Núñez E., Alonso-Torres, P., Fornés A., Aragón C., and López-Corcuera B. (2008) The neuronal glycine transporter GLYT2 associates with membrane rafts: functional modulation by lipid environment. *J. Neurochem.* Postprint' Doi: 10.1111/j.1471-4159.2008.05292.x
44. Apparsundaram, S., Sung, U., Price, R. D. and Blakely, R. D. (2001) Trafficking-dependent and -independent pathways of neurotransmitter transporter regulation differentially involving p38 mitogen-activated protein kinase revealed in studies of insulin modulation of norepinephrine transport in SK-N-SH cells. *J. Pharmacol. Exp. Ther.* **299**, 666-77
45. Moron, J.A., Zakharova, I., Ferrer, J. V., Merrill, G. A., Hope, B., Lafer, E. M., Lin, Z. C., Wang, J. B., Javitch, J. A., Galli, A. and Shippenberg, T. S. (2003) Mitogen-activated protein kinase regulates dopamine transporter surface expression and dopamine transport capacity. *J. Neurosci.* **23**, 8480-8488
46. Zhu, C. B., Hewlett, W. A., Feoktistov, I., Biaggioni, I. and Blakely, R. D. (2004) Adenosine receptor, protein kinase G, and p38 mitogen-activated protein kinase-dependent up-regulation of serotonin transporters involves both transporter trafficking and activation. *Mol Pharmacol.* **65**, 1462-74
47. Samuvel, D. J., Jayanthi, L. D., Bhat, N. R. and Ramamoorthy, S. J. (2005) A role for p38 mitogen-activated protein kinase in the regulation of the serotonin transporter: evidence for distinct cellular mechanisms involved in transporter surface expression. *J Neurosci.* **25**, 29-41
48. Hiroyama, M. and Exton, J. H. (2005) Studies of the roles of ADP-ribosylation factors and phospholipase D in phorbol ester-induced membrane ruffling. *J Cell Physiol.* **202**, 608-22

Legends to figures

Figure 1 GLYT2 traffic is involved in transporter inhibition by PMA. (A) COS7 cells expressing GLYT2 or mock-transfected cells were incubated with vehicle (DMSO) or the indicated PMA concentrations at 18°C or 37°C for 30 min followed by a 5-min incubation at 18°C and a 15-min glycine transport determination at the same temperature (A) or surface biotinylation at 4°C in steady-state conditions (B). (A) Data are presented as a percentage of control activities, which were 1.06 ± 0.2 and 1.14 ± 0.3 nmol gly/mg prot/15 min. Bars represent S.E.M. of triplicate determinations. (B) Representative GLYT2 immunoblot of non-biotinylated (3µg) and streptavidin-pelleted biotinylated proteins (20µg). GLYT2 appears as a 97 kDa mature protein band and a 75 kDa immature transporter. Immunoblot membranes were reprobbed for calnexin (CNX). (C) Densitometric analysis of the averaged data of three independent Western blots as the shown in (B). Values from PMA treatments were compared with vehicle treatments using Student's *t* test. *Significantly different from vehicle-treated cells, $p < 0.05$.

Figure 2 Effect of monensin on surface expression and glycine transport by GLYT2. COS7 cells expressing GLYT2 or mock-transfected cells were incubated with vehicle, 20 µM monensin (mon), 1µM PMA or both at 37°C during 30 min, extensively washed, and subjected to surface biotinylation at 4°C in steady-state conditions as in Figure 1 (A) or to glycine transport measurement (C). Transport data are presented as a percentage of activity under vehicle treatment (1.185 ± 0.2 nmol gly/mg prot/6 min). Bars represent S.E.M. of four determinations. (B) Densitometric analysis of the averaged data of three independent Western blots as the one shown in (A). *Significantly different from vehicle-treated cells, $p < 0.05$ by ANOVA with Bonferroni's post hoc test. (D) MDCK cells expressing GLYT2 treated with vehicle, monensin or 100 µM chloroquine for 30 min at 37°C were subjected to immunofluorescence for GLYT2 (green fluorescence) and for TfR (red fluorescence).

Figure 3 Effect of PMA on glycine transport and surface expression of GLYT2 wild type and K422E mutant. (A, B) Concentration and time dependence of PMA-induced inhibition of glycine uptake. COS7 cells expressing the indicated transporters or mock-transfected cells were incubated with increasing PMA concentrations during 1 hour at 37°C (A) or with 1µM PMA for 0-60 min (B). After washing, glycine transport

activity was measured. Data are presented as a percentage of control activities, which were 1.46 ± 0.4 and 0.56 ± 0.2 nmol gly/mg prot/6 min for GLYT2 and K422E, respectively. Experimental data were fit by non linear regression analysis. Error bars represent S.E. M. of triplicate determinations in a representative experiment that was repeated three times. (C, D) MDCK cells expressing GLYT2 wild type (C) or K422E mutant (D) fused with the green fluorescent protein were treated with DMSO (vehicle), 1 μ M PMA, 20 μ M monensin (mon) or both, or PMA together with 100 nM okadaic acid (PMA+ok.ac.) or 1 μ M staurosporin (PMA+stau) at 37°C during 30 min, fixed and subjected to confocal microscopy. Some examples of plasma membrane (arrows) or internalized transporter (arrow heads) are shown on the presented representative images.

Figure 4 Effect of PMA on the time course of membrane delivery and intracellular accumulation of GLYT2 transporters. (A, B) Delivery. COS7 cells expressing GLYT2 wild type (A) or mutant (B) were biotinylated at 37°C in the presence of 1 μ M PMA or DMSO (vehicle) during the indicated incubation times (5, 15, 30 min), and equal amount of cell proteins were collected on streptavidin agarose beads and subjected to GLYT2 immunoblot. 30 μ g (GLYT2) or 60 μ g (K422E) of biotinylated protein or 4 μ g of non-biotinylated protein were loaded per lane. Lower graphs show the average data from four experiments analyzed by densitometry. (C, D) Intracellular accumulation. COS7 cells expressing GLYT2 wild type (C) or mutant (D) were surface labeled with cleavable NHS-SS-biotin at 4°C for 20 min and immediately warmed to 37°C to allow internalization for various time periods (5, 15, 30 min) in the presence of 1 μ M PMA or DMSO (vehicle). Cells were then chilled to 4°C, treated with MesNa, and equal amount of cell protein processed as in (A). Initial steady-state levels of surface transporters are assessed by biotinylation at 4°C (lanes 0). 80 μ g (GLYT2) or 120 μ g (K422E) of biotinylated protein or 4 μ g of non-biotinylated protein were loaded per lane. Lower graphs show the average data from 4 experiments analyzed by densitometry. (A,B,C,D) Calnexin immunoreactivity was measured as loading control. Steady-state levels of surface transporters were assessed by biotinylation at 4°C, and cell lysates (5% of the volume) were used for calibration of GLYT2 immunoreactivity (not shown).

Figure 5 Effect of PMA on GLYT2 transporters association with membrane rafts. Wild type (left) or mutant transporter-expressing MDCK cells (right) were treated with DMSO (vehicle) or 1 μ M PMA at 37°C for 30 min and then solubilized with 0.5% Triton X-100 at 4°C during 30 min. Detergent-resistant membranes were separated on a 5-30% sucrose density gradient and the fraction proteins subjected to SDS-PAGE and immunoblotting. Gradient fractions 1-12 (from top to bottom) were probed for: GLYT2, the raft marker protein flotillin-1, and a non-raft protein TfR.

Figure 6 Protein kinase C is involved in GLYT2 inhibition by PMA. (A, B) Acute PMA treatment. COS7 cells expressing the indicated transporters or mock-transfected cells were incubated at 37°C for 30 min with DMSO (vehicle), 1 μ M PMA (A) or the indicated PMA concentrations (B) in the absence or presence of 1 μ M staurosporin (A) or 1 μ M GF109203X (PMA+BIS, B). After washing, glycine transport activity was measured. Data are presented as a percentage of control activities, which were 1.22 ± 0.2 and 0.63 ± 0.2 nmol gly/mg prot/6 min for GLYT2 and K422E, respectively (A) and 1.43 ± 0.1 nmol gly/mg prot/6 min for GLYT2 (B). **(C, D) Chronic PMA treatment.** GLYT2-expressing or mock-transfected COS7 cells were incubated overnight (16h) with 1 μ M PMA in culture medium, washed, acutely treated with vehicle or 1 μ M PMA (C) or 20 μ M monensin (D), extensively washed, and subjected to surface biotinylation at 4°C in steady-state conditions as in Figure 1 (D, inset) or glycine transport determination. Inhibitions by acute PMA (C) or acute monensin (D) are shown as percentage of vehicle-treated cells (1.53 ± 0.3 (C) and 1.47 ± 0.4 (D) nmol gly/mg prot/6 min). **(C, inset)** Western blot α -PKC immunoreactivity reprobed for calnexin indicated an effective α -PKC down regulation by chronic PMA treatment. *Significantly different from vehicle-treated cells, $p < 0.05$ by ANOVA with Bonferroni's post hoc test.

Figure 7 Effect of signaling pathways blockers on GLYT2 transport inhibition by PMA. GLYT2-expressing or mock-transfected COS7 cells were preincubated at 37°C for 30 min with vehicle or the following inhibitors: GF109203X (1 μ M), FTP inhibitor III (100 μ M), Rac1 inhibitor (100 μ M), U0126 (50 μ M), PD98059 (50 μ M), SB203580 (10 μ M), PD169316 (20 μ M), SP600125 (50 μ M), LY292002 (30 μ M), or U73122 (10 μ M), and then subjected to acute 1 μ M PMA treatment at 37°C for 30 min. Control PMA

inhibition was $32 \pm 5\%$ and 100% transport activity was 1.62 ± 0.3 nmol gly/mg prot/6 min. *Significantly different from vehicle-treated cells, $p < 0.05$ by ANOVA with Bonferroni's post hoc test.

Figure 8 Effect of monensin and PMA in brainstem primary neurons and synaptosomes. (A-D) Primary brainstem neurons grown for 16 days in vitro were washed with HBS and treated for 30 min at 37°C with vehicle, 20 μ M monensin (A,B), the indicated concentrations of PMA (C), or 500nM PMA (D). The cells were extensively washed and surface biotinylated at 4°C in steady-state conditions as described in Figure 1 (A) or glycine transport by GLYT2 was measured (B,C, D). 100% transport activity in (C) was 2.01 ± 0.2 nmol gly/mg prot/15 min. (E) Purified synaptosomes were preincubated with vehicle (DMSO) or 1 μ M PMA for 30 min at 37°C, solubilized in 0.5% Triton X-100, fractionated through a sucrose gradient, and fraction proteins subjected to SDS-PAGE and immunoblotting. Gradient fractions 1-12 (from top to bottom) were probed for GLYT2 and the raft marker protein flotillin-1. (F) Average GLYT2 and flotillin-1 immunoreactivities in the Western blots of three independent gradients were analyzed by densitometry. For every protein (GLYT2 and flotillin-1), immunoreactivity in the raft (4-6) and non raft fractions (9-12) was expressed as a percentage of the total protein immunoreactivity in the whole gradient.

Fig. 1 Fornes et al.

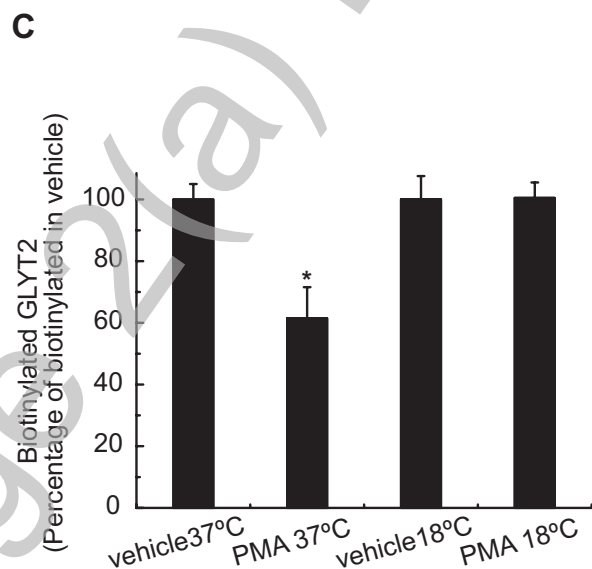
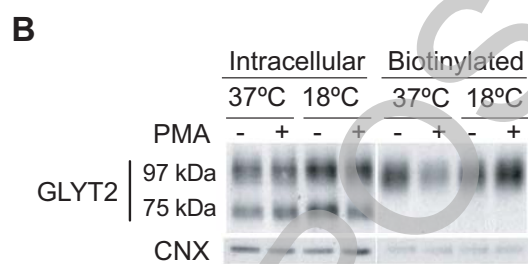
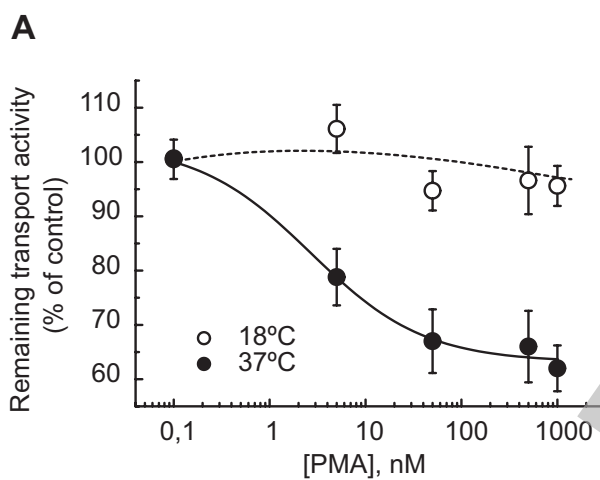


Fig. 2 Fornes et al.

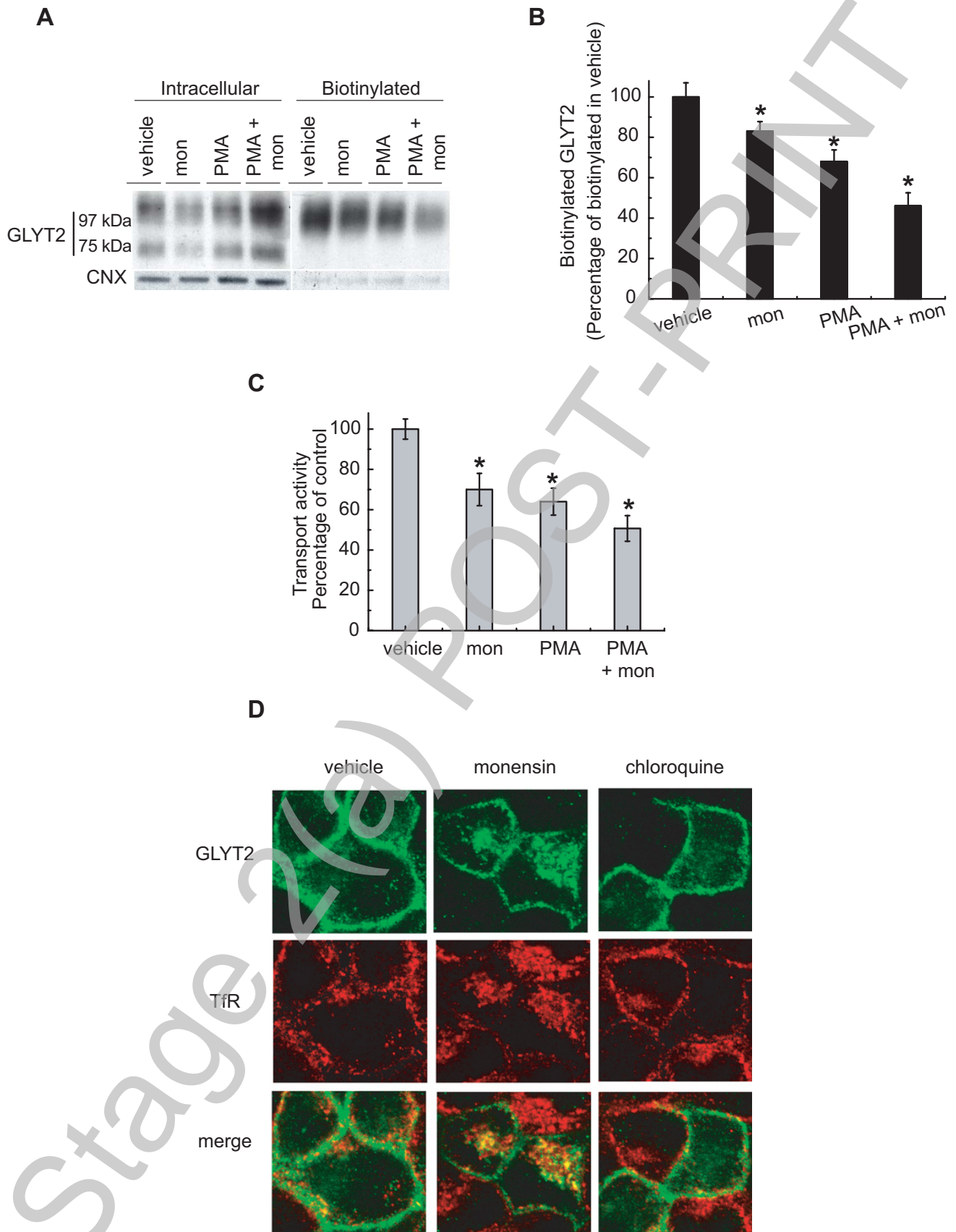


Fig. 3 Fornes et al.

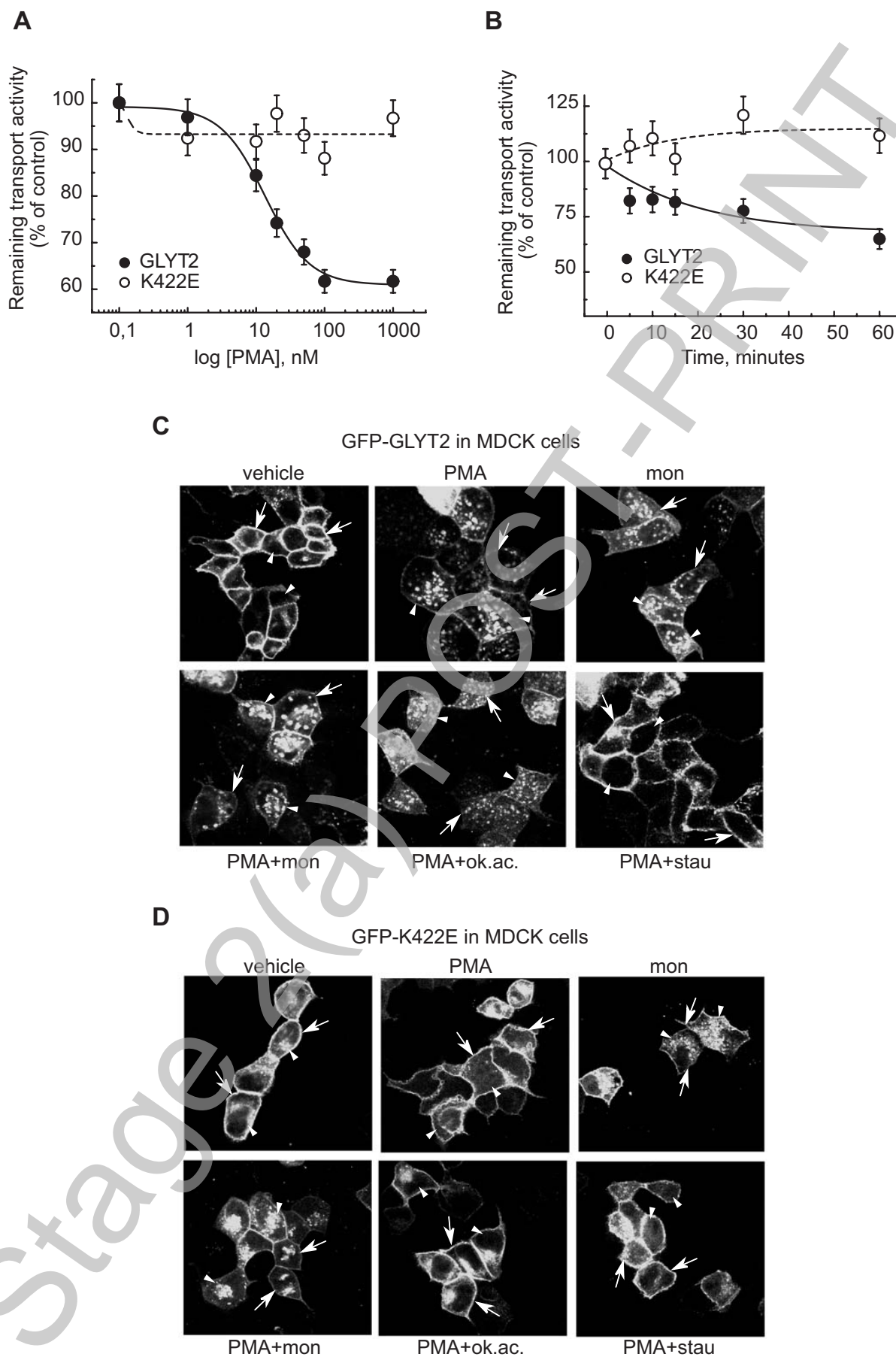
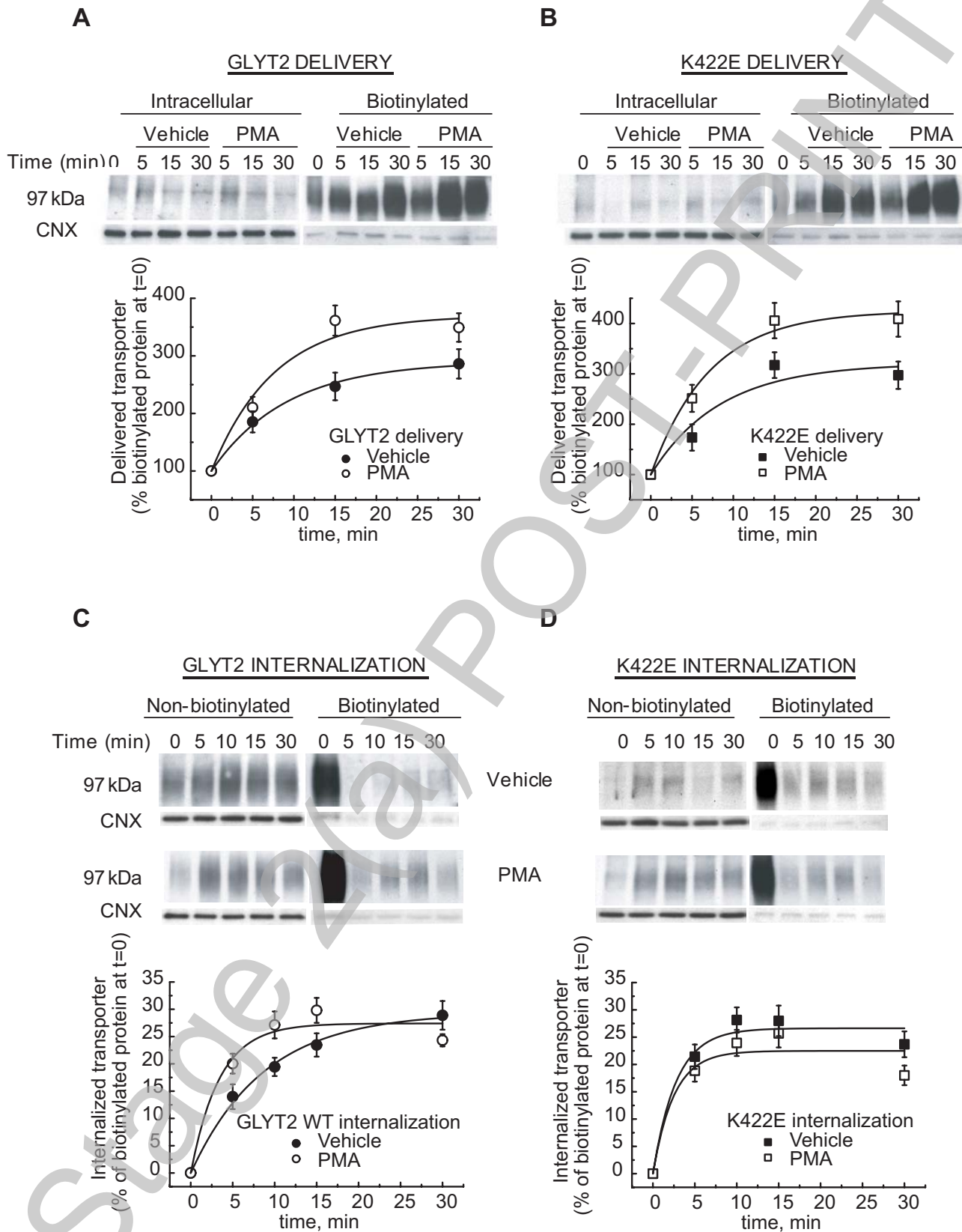
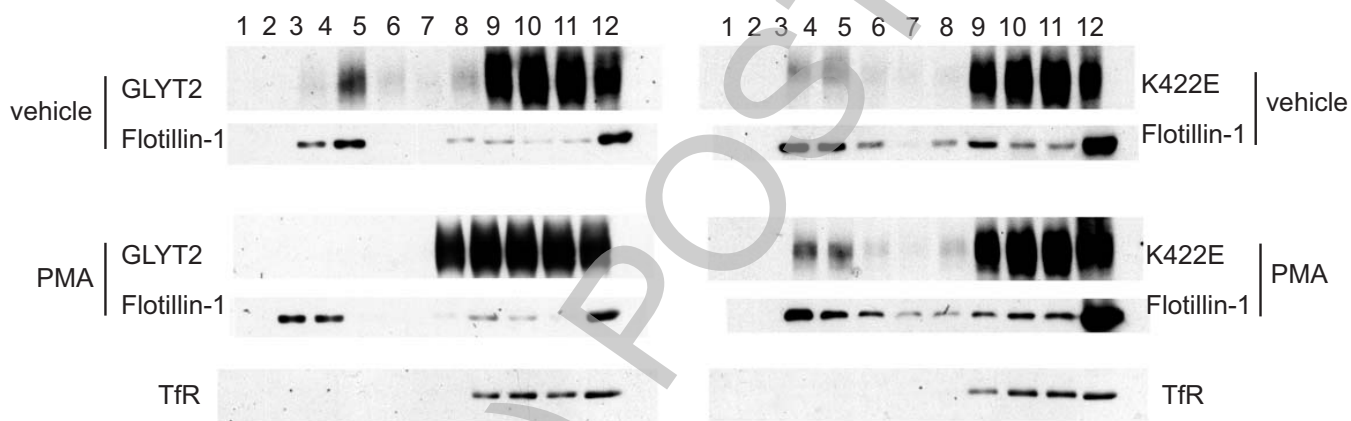


Fig. 4 Fornes et al.



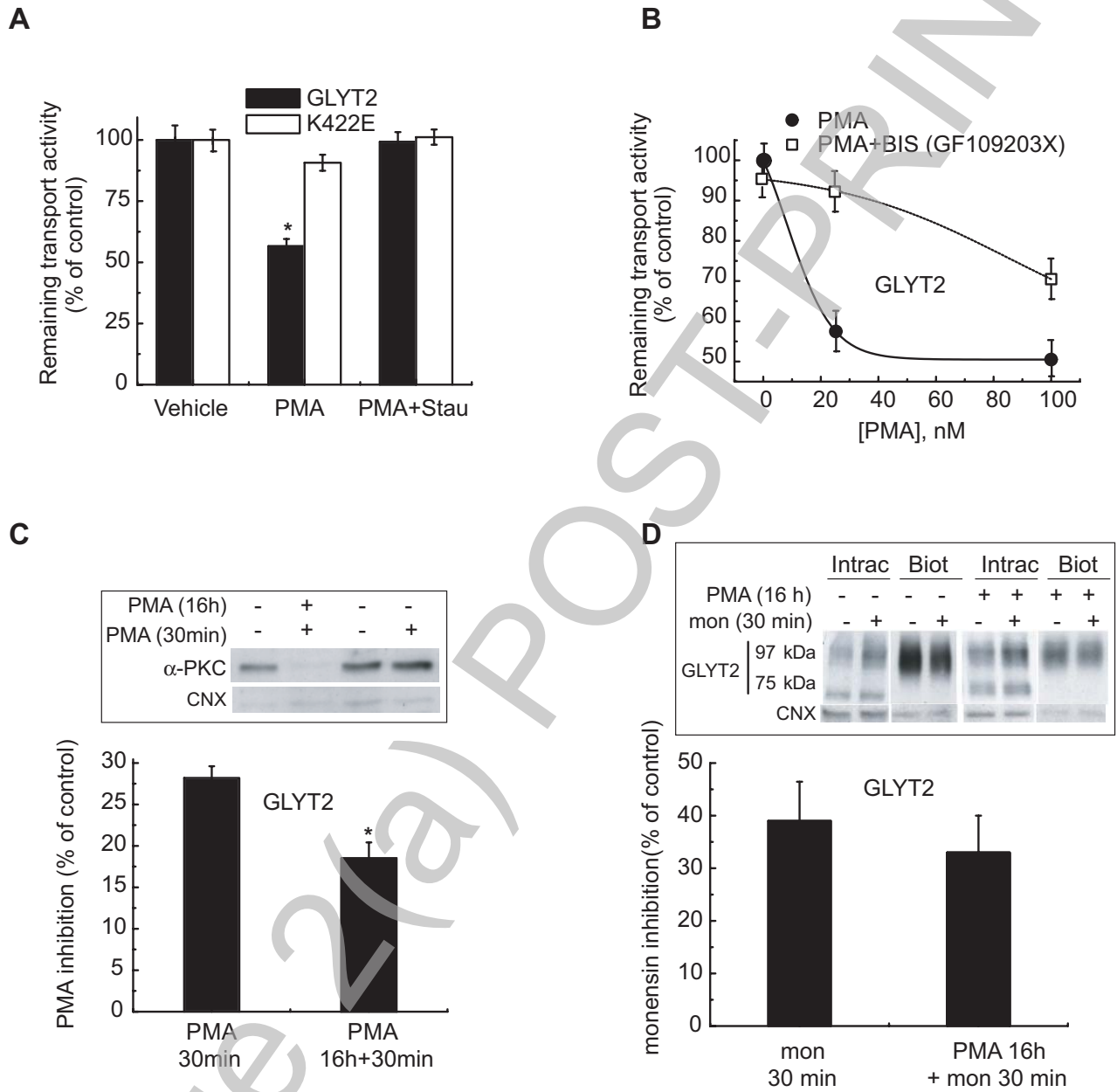
THIS IS NOT THE FINAL VERSION - see doi:10.1042/BJ20071018

Fig. 5 Fornes et al.



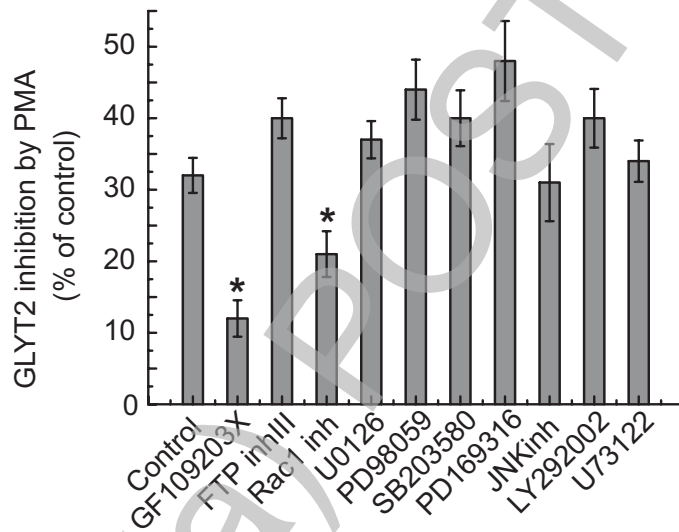
THIS IS NOT THE FINAL VERSION - see doi:10.1042/BJ20071018

Fig. 6 Fornes et al.



THIS IS NOT THE FINAL VERSION - see doi:10.1042/BJ20071018

Fig. 7 Fornes et al.



Stage 2 (a) POST-PRINT

THIS IS NOT THE FINAL VERSION - see doi:10.1042/BJ20071018

Fig. 8 Fornes et al.

